$$I = 0.65 \frac{K}{(1 - K + K^2)} \quad 2.3$$

where,

$$K = \frac{V}{(2Lf)} \quad 2.4$$

by utilizing V as the train speed in ft/s and f as the natural frequency of the loaded bridge in Hz (American 2014). AREMA has suggested that for continuous structures it is a conservative assumption to assume computation of a simple span frequency equation such as:

$$f = \frac{3.5}{\sqrt{\delta}} \quad 2.5$$

where δ is the midspan deflection due to the combination of dead and live load (American 2014).

It can be shown that through application of the equations above and assumptions such as a train speed of 100 mph and a deflection limit of L/750 that for a vast majority of reasonable span lengths, this equation closely follows the current AREMA impact equation:

$$I = \frac{225}{\sqrt{L}} \quad 2.6$$

It should be noted that the impact computation for concrete structures in AREMA is capped at 20% for spans over 127 feet and 60% for spans less than 14 feet. Similarly the steel code portion of AREMA uses the following formulas to compute impacts on steel components:

$$I = 40 - \frac{3L^2}{1600} \quad 2.7$$

for L< 80 feet and:

$$I = 16 + \frac{600}{L - 30} \quad 2.8$$

for L>80 feet (American 2014). An additional 20% may be added to either of these equations where a 'rocking effect' force couple is deemed applicable.

While the Impact formula in Eq. 2.6 above is intended for all concrete bridge types and concrete components and Eqs. 2.7 and 2.8 for all steel bridges, separate impact formulas are intended for box culverts (decreasing linearly from 60% depending on buried depth), 80% impact factor for local steel flange design and 200% for design of direct fixation slab tracks (American 2014).

In comparison, the 2004 Eurocode utilizes two separate 'dynamic factor' equations for rail application depending on the level of track maintenance. The first equation is specifically for projects with "carefully maintained track" and follows:

$$\Phi_2 = \frac{1.44}{\sqrt{L} - 0.2} + 0.82 \quad 2.9$$

where in this case L is in meters and applicable for $1.0 < \Phi < 1.67$ (Eurocode 2004). Similarly, for the default, "standard maintenance" track, the Dynamic Factor is computed by:

$$\Phi_3 = \frac{2.16}{\sqrt{L} - 0.2} + 0.73 \quad 2.10$$

for L in meters and applicable for $1.0 < \Phi < 2.0$ [6]. For the two equations described above, separate impact factors are considered for local and global effects, and separate 'span length' definitions are determined by component type. For continuous structures utilizing the equations above, a portion of the average span length is utilized based on the k factors below:

$$L = kL_{avg} \quad 2.11$$

No. Spans =	2	3	4	>=5
k =	1.2	1.3	1.4	1.5

Although the Eurocode equations described above appears as a straight forward approach, the code requires a list of conditions be met before applicable. These include considerations of train speed, bridge type, span length, as well as the natural bending and torsion frequencies. In most high-speed rail bridge scenarios, Eurocode requires impact factors determined through a dynamic analysis specific to the bridge being analyzed.

2.3 Equation Comparison and Application

Figure 1 below shows a graphical combination of each of the impact factors described above. The general trend for all equations shows the impact as being more critical for short spans. However, AASHTO C4.7.1.1 has noted the potential for increased impact factors for "flexible bridges and long slender components." (AASHTO 2014)

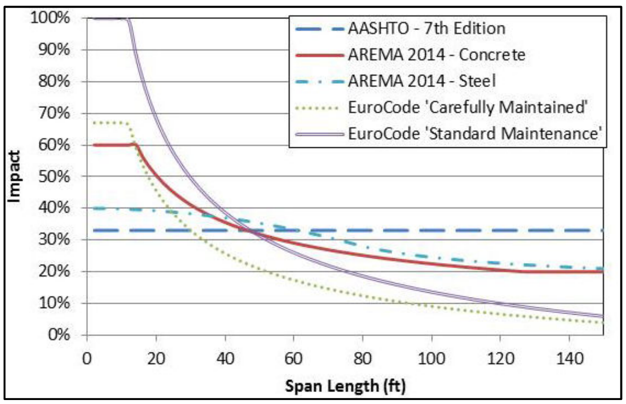

Figure 1. Impact Factor Equations for Current Design Codes

3 DYNAMIC VEHICLE STRUCTURE INTERACTION

To model the dynamic interaction between the vehicle and structure, the vehicle is modeled as a 2D (out-of-plane rotations ignored) rigid multibody system connected by combinations of springs and dampers. The structure is modeled using continuum mechanics and is discretized into finite elements. The equations for the coupled system can be obtained by variational principles. The only major assumption utilized is the computations mandate that when the train is on the bridge the wheels are always in contact with the rail.

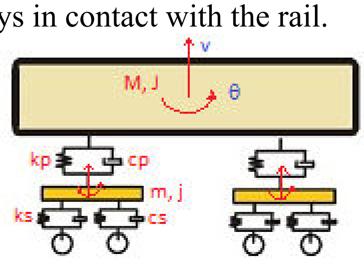

Figure 2. Train Car as a Rigid Multibody System (6 DOF)

3.1 Couple System

Discrete equations for Vehicle-structure are obtained using Euler-Lagrange equations,

$$\frac{\partial V}{\partial U}+\frac{d}{dt}\frac{\partial T}{\partial \dot{U}}=F-\frac{\partial Q}{\partial \dot{U}} \quad 3.1$$

Where, V is the potential energy is the system, T the Kinetic energy of the system, F is the applied force, and Q is the dissipative forces (damping). These are broken down further by:

$$V=\Pi_{bridge}+\Pi_{vehicle},T=T_{bridge}+\mathrm{T}_{vehicle} \quad 3.2$$

Where Π_{bridge} and T_{bridge} are the strain energy of the bridge and $\Pi_{vehicle}$, $T_{vehicle}$ the energy in the train acting as a sprung mass.

By applying Eq. 3.1 on Eq. 3.2 and arranging terms, equations for the coupled vehicle-structure system are obtained. For more detail, see references (Matos 2006), (Yang 2002).

$$\begin{bmatrix} M_{ss} & M_{sv} \\ M_{sv}^T & M_{vv} \end{bmatrix}\begin{bmatrix} \ddot{U}(t) \\ \ddot{W}(t) \end{bmatrix}+\begin{bmatrix} C_s & 0 \\ 0 & C_b \end{bmatrix}\begin{bmatrix} \dot{U}(t) \\ \dot{V}(t) \end{bmatrix}+\begin{bmatrix} K_{ss} & K_{sv} \\ K_{sv}^T & K_{vv} \end{bmatrix}\begin{bmatrix} U(t) \\ W(t) \end{bmatrix}=\begin{bmatrix} f(t) \\ 0 \end{bmatrix} \quad 3.3$$

$$\Psi(t)=\begin{bmatrix} U(t) \\ W(t) \end{bmatrix} \quad 3.4$$

Where $U(t)$ is the structure nodal displacements and $W(t)$ the train displacements. K_{sv} is the term that couples the train and the bridge and depends on the location of the train. Some researchers (Yang 2002), (Yau 1999) set this term in the right-hand-side of Eq. 3.3, to consider $K_{sv}W(t)$ as the interaction force.

$$M(t)\ddot{\Psi}(t)+C(t)\dot{\Psi}(t)+K(t)\Psi(t)=P(t) \quad 3.5$$

To solve Eq. 3.5 it is important to consider that the train is traveling at high speeds and can cross most bridge lengths in just a few seconds. Impact factors have to capture peak values of displacement; thus the transient response cannot be ignored.

3.2 Structure

The stiffness matrix for structure obtained using Eq. 3.1 depends on the finite element used. For beam elements a 3-D 12 DOF, Bernoulli element was used. Comparatively for shells, a bilinear 6 DOF per node (capable of sustain finite-strains and finite rotations) was used, see references (Simo 1989) and (Simo 1990) for details of elements. These elements were implemented in Multiphysica (Multiphysica 2016). Lumped mass matrix was used to reduce the computational effort, without loss of precision. The damping matrix was explicitly required to integrate equations. Therefore, the Rayleigh damping matrix was used

$$C_s=a_0M_{ss}+a_1K_{ss} \quad 3.6$$

with coefficients a_0 and a_1 dependent on a critical dumping of 1 percent assumed for the two periods of the structure.

$$a_0=\frac{4\pi\xi}{T_1},\ a_1=\frac{1}{\pi}\frac{T_1T_2\xi}{T_1+T_2} \quad 3.7$$

3.3 Vehicles

Using equations 3.1 and 3.2, stiffness, mass and damping matrix were derived. Eq. 3.8 was derived strictly for the topology of train described in Fig. 2. This numerical representation of the train was described by Yang (Wu 2001) and is widely used for high speed rail analysis. Five types of trains with similar topology but different lengths, different wheel spacing, different weight distributions, and a different number of cars per train were studied. Table 1 describes these five variants of trains.

$$K_{vv} = \begin{bmatrix} 2k_s & 0 & -k_s & -k_s & 0 & 0 \\ 0 & 2a^2k_s & -ak_s & ak_s & 0 & 0 \\ -k_s & -ak_s & k_s + 2k_p & 0 & 0 & 0 \\ -k_s & ak_s & 0 & k_s + 2k_p & 0 & 0 \\ 0 & 0 & 0 & 0 & 2s^2k_p & 0 \\ 0 & 0 & 0 & 0 & 0 & 2s^2k_p \end{bmatrix}, M_{ss} = \begin{bmatrix} M_s \\ J_c \\ m_f \\ m_f \\ J_b \\ J_b \end{bmatrix} \quad 3.8$$

3.4 Numerical Integration

Several computational methods were considered for the integration of time history equations to ensure the use of a robust and stable method. Bathe (Bathe 2005), (Bathe 2012) showed that methods stable under linear conditions can fail under non-linear conditions. The Central Difference method works only for short intervals of time (small spans and/or train with maximum a couple cars). The Wilson Theta method was an unconditional stable method, but failed for trains with multiple cars. Therefore, realistic situations (long span bridges and 8 to 12-train car scenarios) were solved with the Hilber-Hughes-Taylor (Hilber 1977) (HHT) method.

HHT is an implicit method, thus each time step requires iterations. HHT is unconditionally stable, so the size of time step does not affect convergence. The time step (Δt) chosen for analysis was selected only to have enough resolution of displacements (U).

$$U_{n+1} = U_n + \Delta t\dot{U}_n + [(0.5-\beta)\Delta t^2]\ddot{U}_n + \beta\Delta t^2\ddot{U}_{n+1} \quad 3.9$$

$$\dot{U}_{n+1} = \dot{U}_n + [(1-\gamma)\Delta t]\ddot{U}_n + \gamma\Delta t\ddot{U}_{n+1} \quad 3.10$$

$$\beta = \frac{(2-\alpha)^2}{4}, \gamma = \frac{3}{2} - \alpha \quad 3.11$$

$$\frac{2}{3} \le \alpha \le 1 \quad 3.12$$

For all computations of the VSI, a value of $\alpha = 0.995$ was used, therefore the numerical damping introduced by HHT was rather minimal.

Table 1. Trainset Properties (US Customary Units k,ft) (Wu 2001)

TRAIN PROPERTIES		CAHSR				
		LLV-1	LLV-2	LLV-3	LLV-4	LLV-5
	Number of cars	8	8	10	8	8
Dimensions	Bogies distance	57.1	57.4	57.4	57.4	57
	From bogie to end	30.2	24.6	24.6	24.6	22.4
	Spacing of wheels	8.9	8.2	8.2	8.2	8.2
	Total length	87.3	82	82	82	79.4
Mass	Car body	120.8	103.2	70.4	94.4	120.8
	Car pitch	64761	55323	37734	50604	64761
	Bogie	6.70	6.70	6.70	6.70	6.70
	Bogie pitch	93	93	93	93	93
	Bogie Wheels	3.86	3.86	3.86	3.86	3.86
Stiffness	Primary	80.91	80.91	80.91	80.91	80.91
	Secondary	36.34	36.34	36.34	36.34	36.34
Damping	Primary	2.69	2.69	2.69	2.69	2.69
	Secondary	6.18	6.18	6.18	6.18	6.18

4 BRIDGE MODELS AND PROCEDURES USED

4.1 Bridge Types

Nine different structures were considered for the study of vehicle-structure interaction. The preferred structure type was a single-cell concrete box with simple span lengths of 60 feet and 120 feet which will be further referred to as the 60ft_box and the 120ft_box respectively. The same cross section was considered for a 3 span (90ft - 120ft – 90ft) continuous (referred to as 3_span_box) as well as a continuous option over straddle bents (referred to as box_over_straddle_bents). A prestressed beam bridge of 8- CA WF48 girders spanning 60' in a simple span arrangement was also considered (referred to as PS_beam). The sixth bridge considered was a concrete through girder option spanning a single 120' span. Additionally a 'pergola' structure was considered of 4-60' spans continuous in the longitudinal direction with CA WF84 girders spanning 116' in the transverse direction at 5' spacing. The final concrete option studied was a concrete box culvert with an top slab span length of 40' and a box height of 20'. The single steel option considered was a 175' simple span steel truss.

4.2 Box Geometry

The box girder was modelled with 2' thick webs and was 12' deep from top of bearing to top of slab. The top slab was 43' wide and sloped towards a deck drain in the center on a 2% slope. The top slab varied in thickness from 1' to 1.25' and bottom slab was a constant 1.5' thick. The box girder was designed for multiple post tensioned strands to be draped within each web of the box. Post tensioning effects were not considered in our analysis, nor were they modelled. The box section was modelled using shell elements with a maximum mesh size of 5'.

4.3 Prestressed Beam Bridge

The deck girder option was a 60' span with eight CA WF48 prestressed, precast girders. The deck surface was finished with a 9" composite slab. The girders were modelled as frame elements with rigid link connections to the shell elements of the deck. Concrete diaphragms 1.5' wide x 2.5' deep were modelled between all beams at the ends and third points of the structure.

4.4 Through Girder

The through girder was designed with two 3.75' wide by 16' tall concrete walls separated by 45.5'. The girders were modelled as frame elements at the same level as the deck surface and offset upwards to the centroid of the beam. The slab of the U-shaped through girder was a 3.75' thick deck modelled as shell elements and directly supported the rail loads. Post tensioning utilized for strength was not used in this analysis.

4.5 Pergola Structure

The pergola was generated with two continuous edge beams of 6' deep x 6' wide concrete frame elements with direct fixations to the columns. These edge beams supported transverse CA WF84 beams on 5' intervals for the entirety of the modelled structure. A deck surface of 8" thick was composite with the transverse beams and directly supported the rail which was running at a slight skew of about 4 degrees relative to the bridge.

4.6 Box Culvert

The concrete box culvert was modelled with the bottom slab, walls, and top slab all 3.5' thick. The rail was placed on the top slab at a skew angle of nearly 35 degrees, and therefore 'counter-fort' extensions were added on either side of the box to make the start and of bridge begin perpendicular to the rail. No foundation springs were modelled, but instead the 4 corners were pinned in location as a conservative, under approximation of support stiffness.

4.7 Steel Truss

The truss was modelled as a Warren Truss with five panels each 35' deep and 35' wide. The two primary truss walls were separated by 44' with transverse bracing on the top of the truss and portal bracing at each truss point. Additional end verticals were provided as a secondary load path in the event of vehicular collision of the entrance portal. The truss diagonals and vertical end posts were all 2' deep steel I-sections and small W14 sections were used to create all transverse bracing. Steel Box sections 3' deep x 2' wide were used for the top chord with similar sections 4' deep used for the bottom chord. The truss supported 17 equally spaced I-shaped floor beams of 3.5' depth acting compositely with a 1' thick concrete deck.

4.8 Materials

All superstructure concrete was modelled as 6000 psi normal weight concrete and substructure concrete was 5000 psi. Material exceptions were the Box Culvert and Through Girder which used 4000 psi concrete and the pergola structure which used 9000 psi concrete for the prestressed beams. The steel truss was modelled with A992Fy50 grade steel.

4.9 Substructure Assumptions

For consistency of results, all bridges were modelled as 30 feet above ground on hammerhead piers with 9' diameter or 9' square columns. The only exception was the straddle bent model which consisted of two 6.5' diameter columns per bent. For modeling simplification, the columns were assumed fixed at the base and no foundations or soil related springs were modeled in this analysis.

4.10 Track Modelling

The rail was modeled as a line element directly on the deck surface and vertical loads directly applied for both the static and dynamic cases. No rail-interaction, namely rail springs, were used in the analysis completed. All bridges were designed for a two track system with each track centered 8.25' on either side of the CL of the structure. The exception was the pergola structure with which the track line was splayed from one corner of the structure to the other to allow for a skew between the passing train overhead and the clearance required below. Only one loaded track was considered.

4.11 Bearings and Connection to Substructure

Fixed bearings were assumed to be fixed for translation in all directions and free to allow for rotation between the superstructure and substructure. Roller bearings were similar but allowed for translation longitudinal to the bridge. Simple span structures modeled assumed one end on fixed bearings and the other end on roller bearings. Continuous structures had fixed bearings on interior piers and roller bearings on end piers. No bearings were used in the Pergola nor Box Culvert structures as the superstructure and substructure were direct fixations.

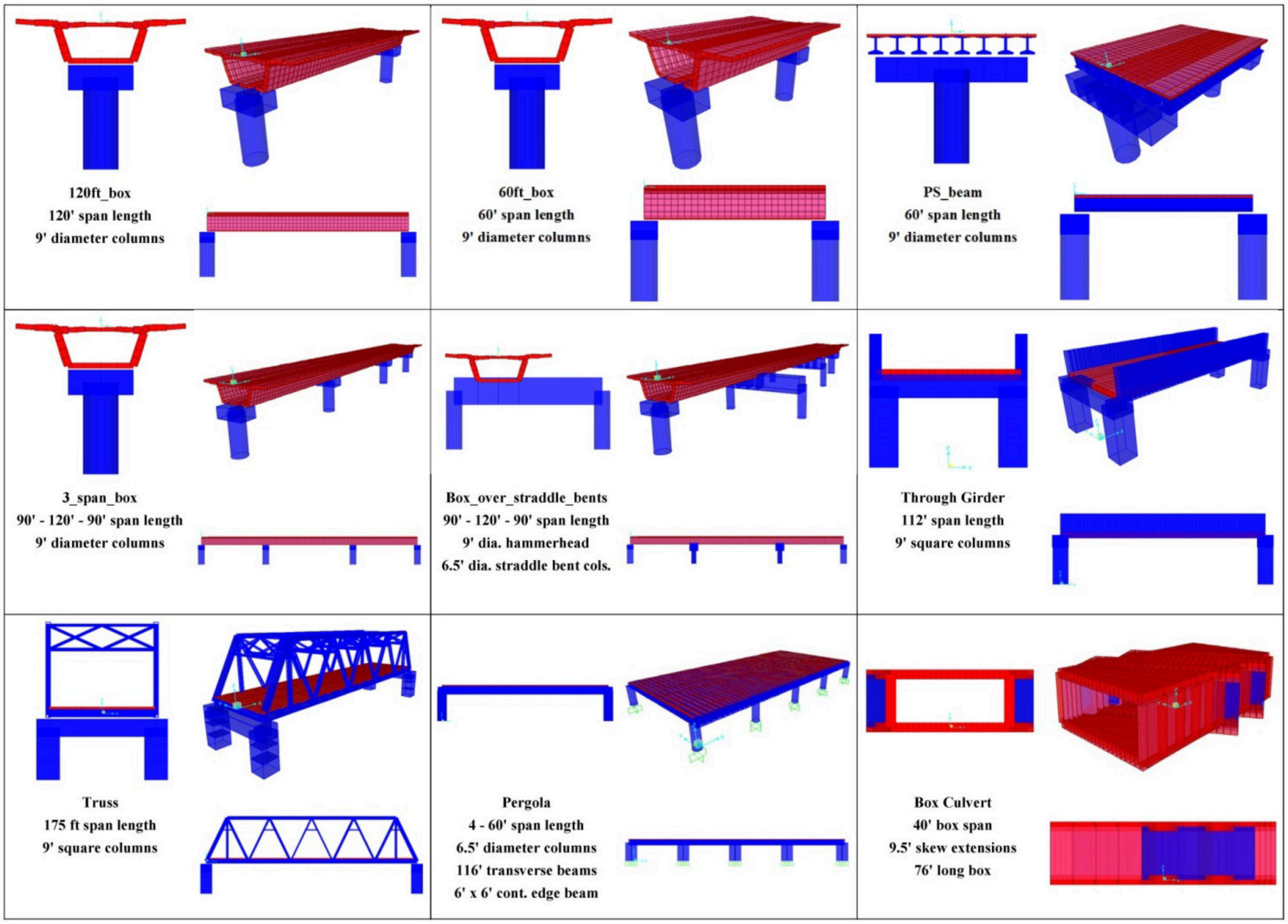

Figure 3. Bridges used in Modelling (frame elements – blue, shell elements – red)

4.12 Modelling Programs and Analysis

A combination of finite element programs were used for modelling, analysis, and verification of results for the dynamic analysis both with and without the vehicle interaction. CSI Bridge, SAP2000, and a proprietary software, Multiphysica, were used for analysis of all nine bridges considered.

Eigenvalue analysis was utilized to verify the modal behavior of the structure, and results recorded for determining the Rayleigh damping coefficients.

Multi-step static analysis was performed to determine the deflected shape of the structure under each train position, and a time history analysis was similarly performed to capture the dynamic behavior at each step.

4.13 Moving Mass Approximation

The mass of all structures included self-weight as well as an additional nodal mass to represent the additional dead load due to ballast, parapet, and overhead catenary systems. In the vehicle-structure interaction, the mass of the train was simulated by an equivalent moving mass applied at each axel position. However, for the dynamic analysis without vehicle interaction, the train was modeled as moving loads and an effective mass was applied nodally on the deck surface. This effective mass was the average train mass of the five trains considered and was evenly distributed across the loaded train path. The train speeds which were analyzed for dynamic analysis, varied from 90mph to 250 mph in 10 mph increments.

4.14 Location of Deflection Points

Dynamic and static deflections were considered under rail locations on the deck surface. The absolute deflection due to superstructure bending, superstructure shear deformation, substructure deformations, and local slab deflections were considered in both the static and dynamic cases. Amplification due to local effects were considered as these effects will realistically affect the response of the train.

5 RESULTS

Fig. 4 depicts the variation of the static and dynamic displacement (measured at center span of the bridge) with the position of the train, for the 120ft_box when train type LLV-3 crosses at a speed of 250 mph. After all train cars have crossed the bridge, the response is a free vibration, which was damped out in a few seconds. Fig. 5 is similar to Fig. 4, but in this case the interaction vehicle-structure has been included in the analysis. This case is also for the 120ft_box under train type LLV-3 crossing at 250 mph.

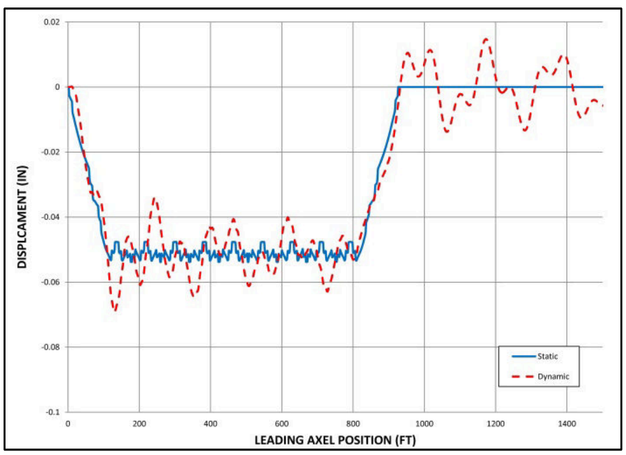

Figure 4. Displacement of center node for 120ft_box for LLV3 at 250 mph with no interaction considered

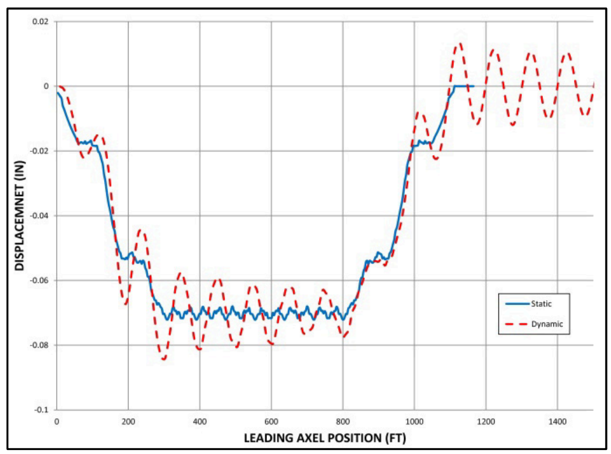

Figure 5. Displacement of center node for 120ft_box for LLV3 at 250 mph with interaction considered

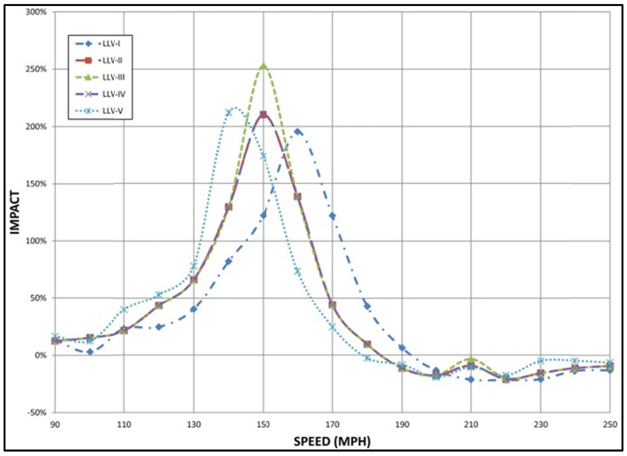

Figure 6. Impact Factor computation for 60ft_box interaction not considered

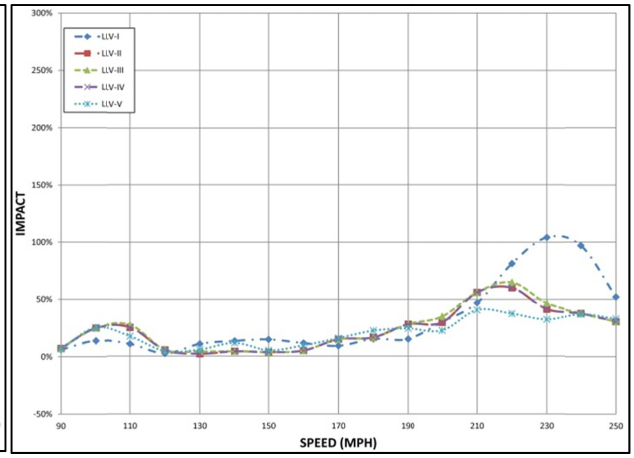

Figure 7. Impact Factor computation for 60ft_box with interaction considered

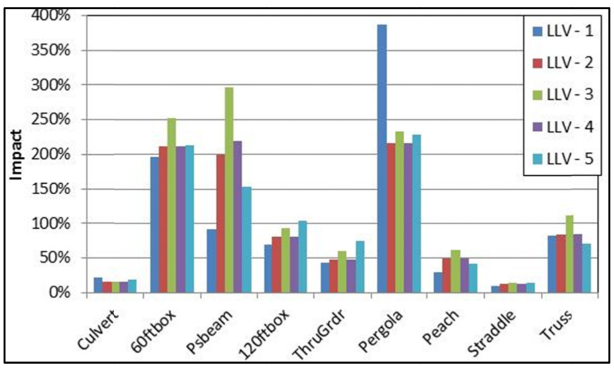

Figure 8. Impact Factors with No Interaction

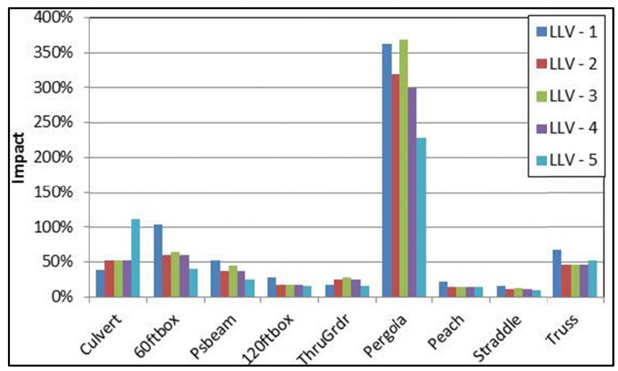

Figure 9. Impact Factors with Interaction

Fig. 6 describes the variation of impact factor with the speed for the 60’ box girder. It can be seen, that peak values occur at different speeds for the different types of trains studied. Fig. 7, also describes the variation of impact factor for a range of speeds, but in this case VSI was included, and corresponds to the same 60ft box girder. It can be reasoned that peak values are smaller than the ones depicted in Fig. 6. This clearly shows the importance of performing VSI analysis to compute impact factors. Velocities corresponding to peak values are quite different from the first resonance velocities shown in Table 3. However, these theoretical resonance speeds were derivate from over simplified 1-D systems, which do not consider substructure, nor other complexities, considered in the finite modeling of the bridges studied.

Fig. 8 shows the maximum impact factor for the different bridges studied for each of the five types of trains analyzed. In general, shorter span bridges have higher impact factors than longer span bridges studied. The Pergola Type Bridge was the exception where large impact factors were computed. In this unique case, this is likely related to the fact that the transverse span is longer than the longitudinal span. Similarly, Fig. 9 shows impact factors, but in this case the

Vehicle-structure interaction was included. Similar trends found above were present for VSI. The same general trend of VSI greatly reducing the impact factor was present with the case of the culvert being a unique exception.

Table 2, summarizes results of impacts, primary frequencies and maximum static displacements. It can be seen that displacements are quite small to satisfy stringent high speed rail deflection requirements.

Table 2. Summary of Impact Results

	Impact		1st frequency	Max Static Deflection
	w/o interaction (%)	w/ Interaction (%)	(Hz)	(in)
Box Culvert	20.8	52.5	5.89	0.0003
60ft_box	253.0	104.2	2.91	0.0307
PS_beam	296.8	52.2	3.65	0.0560
120ft_box	103.8	27.4	2.01	0.0940
Through Girder	74.9	27.2	7.27	0.0210
Pergola	386.7	369.4	2.36	0.2680
3_span_box	61.5	21.7	1.91	0.0590
Box_over_straddle_bents	14.6	14.8	1.45	0.0420
Truss	112.6	67.1	3.00	0.1620

Table 3. Resonance Speeds

	First Resonance Speed (mph)				
	LLV1	LLV2	LLV3	LLV4	LLV5
Box Culvert	751	705	705	705	682
60ft_box	809	759	759	759	734
PS_beam	525	493	493	493	477
120ft_box	292	274	274	274	265
Through Girder	256	241	241	241	233
Pergola	228	214	214	214	207
3_span_box	Resonance Not Computed				
Box_over_straddle_bents	for Continuous Span Structures				
Truss	226	212	212	212	205

6 CONCLUSIONS AND RECOMMENDATIONS

3-D models utilizing a combination of shell and beam elements to capture a high level of detail can be computationally very demanding to capture impact factors via transient dynamic analysis. From the results for both cases with and without VSI described in the previous section, several key conclusions can be listed:

- Impact factors computed by dynamic analysis are much larger than impact factors used by AREMA or AASHTO.
- For the current engineering practice VSI requires large computational effort.
- Shorter span bridges have larger impact factors.
- Inclusion of the Vehicle-structure interaction produces smaller impact factors.
- Vehicle speed corresponding to the maximum impact factor shifts when VSI is considered.